

This article was downloaded by:

On: 22 January 2011

Access details: *Access Details: Free Access*

Publisher *Taylor & Francis*

Informa Ltd Registered in England and Wales Registered Number: 1072954 Registered office: Mortimer House, 37-41 Mortimer Street, London W1T 3JH, UK



The Journal of Adhesion

Publication details, including instructions for authors and subscription information:

<http://www.informaworld.com/smpp/title~content=t713453635>

Development of a Failure Model for the Adhesively Bonded Tubular Single Lap Joint

Su Jeong Lee^a; Dai Gil Lee^a

^a Department of Precision Engineering and Mechatronics, Korea Advanced Institute of Science and Technology, Daejeon, Korea

To cite this Article Lee, Su Jeong and Lee, Dai Gil(1992) 'Development of a Failure Model for the Adhesively Bonded Tubular Single Lap Joint', *The Journal of Adhesion*, 40: 1, 1 – 14

To link to this Article: DOI: 10.1080/00218469208030467

URL: <http://dx.doi.org/10.1080/00218469208030467>

PLEASE SCROLL DOWN FOR ARTICLE

Full terms and conditions of use: <http://www.informaworld.com/terms-and-conditions-of-access.pdf>

This article may be used for research, teaching and private study purposes. Any substantial or systematic reproduction, re-distribution, re-selling, loan or sub-licensing, systematic supply or distribution in any form to anyone is expressly forbidden.

The publisher does not give any warranty express or implied or make any representation that the contents will be complete or accurate or up to date. The accuracy of any instructions, formulae and drug doses should be independently verified with primary sources. The publisher shall not be liable for any loss, actions, claims, proceedings, demand or costs or damages whatsoever or howsoever caused arising directly or indirectly in connection with or arising out of the use of this material.

Development of a Failure Model for the Adhesively Bonded Tubular Single Lap Joint

SU JEONG LEE and DAI GIL LEE

Department of Precision Engineering and Mechatronics, Korea Advanced Institute of Science and Technology, Daejeon, Korea, 305-701

(Received April 6, 1992; in final form June 11, 1992)

The accurate calculation of the stresses and torque capacities of adhesively bonded joints is not possible without understanding the failure phenomena of the adhesive joints and the nonlinear behavior of the adhesive.

In this paper, an adhesive failure model of the adhesively bonded tubular single lap joint with steel-steel adherends was proposed to predict the torque capacity accurately.

The model incorporated the nonlinear behavior of the adhesive and the different failure modes in which the adhesive failure mode changed from bulk shear failure, *via* transient failure, to interfacial failure between the adhesive and the adherend, according to the magnitudes of the residual thermally-induced stresses from fabrication.

KEY WORDS adhesion; adhesive failure model; adhesive layer thickness; stresses and torque capacities; transient failure mode; nonlinear mechanical behavior; thermally-induced residual stresses from fabrication; steel adherends; rubber-toughened epoxy adhesive; theory; experiment; torsional strength.

INTRODUCTION

The design of the joint in the assembly of separated parts has become an important research area, because the structural efficiency of the structure is established, with few exceptions, by its joints and not by its basic structure.

There are two kinds of joints: mechanical and bonded. Adhesively bonded joints enable the distribution of the load over a larger area than mechanical joints, require no hole, add very little weight to the structure, and have superior fatigue resistance. In this work, the analysis was confined to the adhesively bonded joints, even though they require careful surface treatments of the adherends, are affected by service environments, and are difficult to disassemble for inspection and repair.

There are several types of adhesive joints, such as the single lap joint, the double lap joint, the stepped lap joint, and the scarf joint. Among these, the single lap joint is most popular, due to its ease of manufacture and its relatively low cost. However, the single lap joint produces relatively high stress concentration in the end region of the adhesive and, consequently, low load transfer capacity. To overcome these disadvantages of the single lap joint, other joints, such as the double lap, the stepped and the scarf were devised by several researchers.

Stress analyses on tubular lap joints, especially on the single lap joint, have been

conducted extensively by many researchers using analytical and finite element methods.

Alwar and Nagaraja¹ used a finite element method to obtain the stresses in the tubular single lap joint subjected to torsion. The time-dependent properties of the adhesive were considered in this finite element method.

Adams and Peppiatt² refined the solution of Volkersen³ and gave a closed-form solution for the shear stresses in tubular single lap joints and partially-tapered tubular scarf joints. He also analyzed adhesive tubular lap joints which were subjected to axial and torsional loads using a finite element method when the adhesive had a fillet.

Chon⁴ analyzed, in closed form, the adhesive tubular single lap joint whose adherends were composite materials by a method similar to that of Adams.

Hipol⁵ analyzed a tubular lap joint comprised of a steel tube which was adhesively bonded to a composite tube and subjected to torsion. He used a finite element method to characterize the stress concentration associated with the boundary layer effect in the end region of the adhesive layer. He concluded that the stress reduction effect was only marginal when the steel adherend was partially tapered.

Graves and Adams⁶ used a finite element method to calculate the stresses of a tubular single lap joint whose adherends were orthotropic composite material subjected to torsion. He obtained the stresses in the adherends by a ply-by-ply analysis. Also, he obtained the stresses in the adherends with smeared laminate properties.

Hart-Smith⁷ analyzed several adhesively bonded joints such as the double lap, the single lap, the scarf, and the stepped lap joint and developed computer software for the analysis.

Thomsen and Kildegaard⁸ used the nonlinear material properties of the adhesive for a more realistic approach in the analysis of adhesively bonded, generally orthotropic, circular cylindrical shells under complex loadings.

Lee *et al.*⁹ experimentally investigated the effect of the adhesive thickness and the adherend roughness on the torsional fatigue strength of adhesively bonded tubular single lap joints.

As mentioned before, many researchers have analyzed the stresses and the torque capacities of adhesively bonded tubular lap joints and the related references are abundant.^{10,11,12} However, the previously-published calculation schemes could not predict accurately the torque capacity of the adhesively bonded tubular lap joint unless they were modified to incorporate the nonlinear behavior of the adhesives and different failure modes according to the adhesive thickness.

In this paper, therefore, the static torque capacity of the adhesively bonded tubular single lap joint was investigated experimentally and theoretically with respect to the adhesive layer thickness. In order to match the calculated torque capacity of the joint to the experimentally-determined one, the failure model of the adhesive was proposed according to the magnitude of the fabrication thermal residual stresses which were functions of the adhesive layer thickness and the size of the joint. The model assumed that the failure mode changed from bulk shear, *via* a transient, to interfacial failure between the adhesive and the adherend as the magnitude of the thermally-induced residual stresses from fabrication increased.

EXPERIMENTAL

The torque capacity of the adhesively bonded tubular lap joint depends heavily on the adhesive thickness. The closed form² and the finite element calculation⁵ predicted that the torque capacity of the joint increased as the adhesive thickness increased, which was usually contrary to the experimental test results.

In this paper, the adhesively bonded tubular single lap joints with steel-steel adherends were statically tested under torsion to investigate the dependency of the torque capacity on the adhesive thickness. The adhesive used was a rubber-toughened epoxy. Table I shows the mechanical properties of the adhesive and the steel adherend and Figure 1 shows the shear stress-strain relation obtained by the torsion test. From Figure 1, we can see the large plastic deformation of the adhesive beyond the yield stress which is the typical characteristic of the rubber-toughened epoxy adhesive material.

The configuration of the adhesive bonded tubular single lap joint is depicted in Figure 2. The adhesive bonding thickness was controlled by changing the diameter of the inner adherend while the diameter of the outer adherend was fixed. Both the inner adherend and the outer adherend have accurate mounting surfaces which were ground, and the concentricity between the outer and the inner adherends was secured by mounting the ground surfaces in an accurate V-block when curing the adhesive. Steel adherends rather than composite adherends were chosen because close control of the dimensions and roughnesses of the steel adherends was simple. The arithmetic surface roughness of $2\mu\text{m}$ was chosen for the adherend surface roughness because this value was proved to be the optimum for the fatigue strength of the same testpiece.⁹

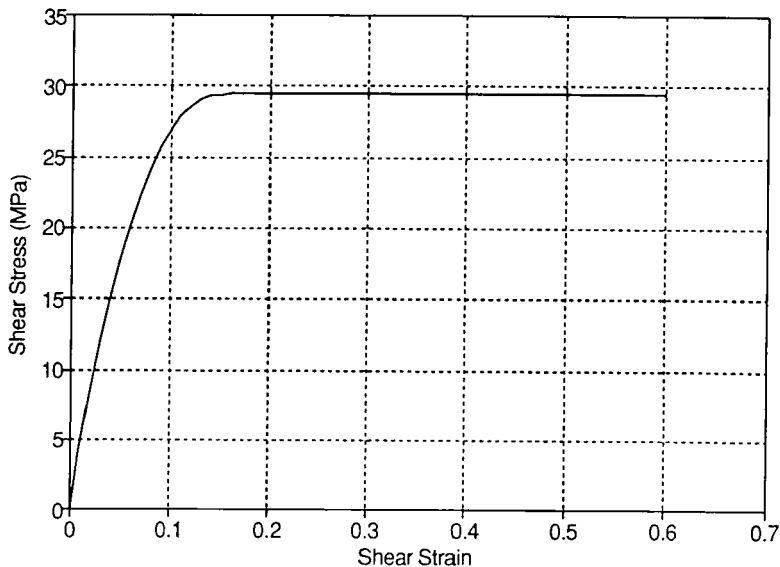


FIGURE 1 Shear stress-strain curve of the epoxy adhesive (IPCO 9923).

TABLE I
Material data for the epoxy adhesive and the steel adherend

	Adhesive IPCO 9923*	Adherend steel
Tensile modulus (GPa)	1.30	200.0
Shear modulus (GPa)	0.461	76.9
Poisson's ratio	0.41	0.30
Tensile strength (MPa)	45.0	Not required
Shear strength (MPa)	29.5	Not applicable
Shear strain limit	0.60	Not required
Thermal expansion coefficient (10^{-6} m/m °C)	72.0	11.7
Viscosity	Paste type	Not applicable
Cure temperature (°C)	80.0	Not applicable
Cure time (hour)	3	Not applicable

*Imperial Polychemicals Corporation, Azusa, CA 91702, U.S.A.

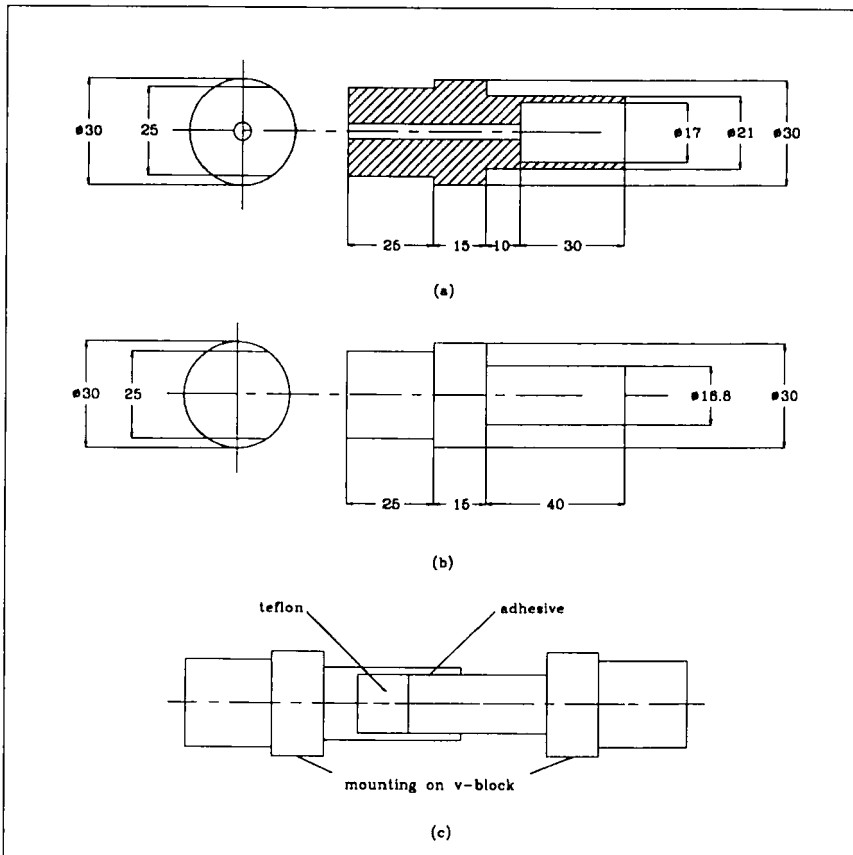


FIGURE 2 Configuration of the adhesively bonded joint specimen. (a) Outer adherend; (b) Inner adherend; (c) Adhesively bonded joint.

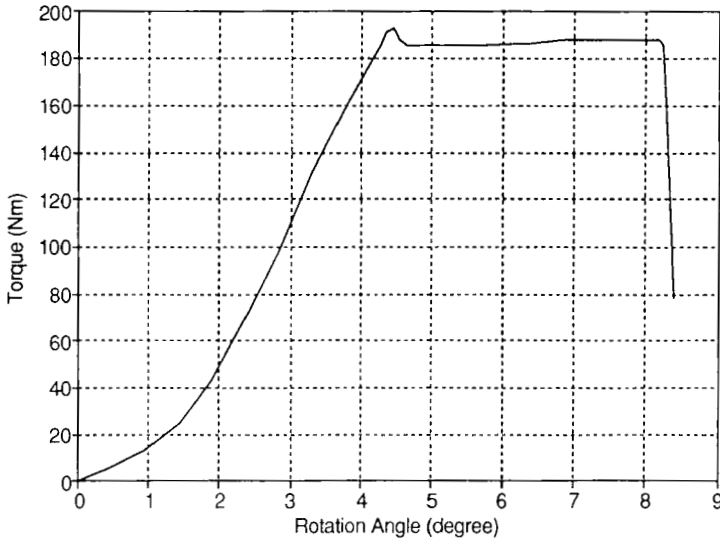


FIGURE 3 Static torsion test result of the adhesively bonded joint specimen (Bonded thickness = 0.1 mm).

The joint specimens were cured in an autoclave such that the temperature was 80°C, the pressure was 0.6 MPa and the curing time was 3 hours.

Figure 3 shows the static torsion test results when the bonding thickness was 0.1 mm. There is large torque saturation region when the relative rotation of the steel adherends was larger than 4.5 degree.

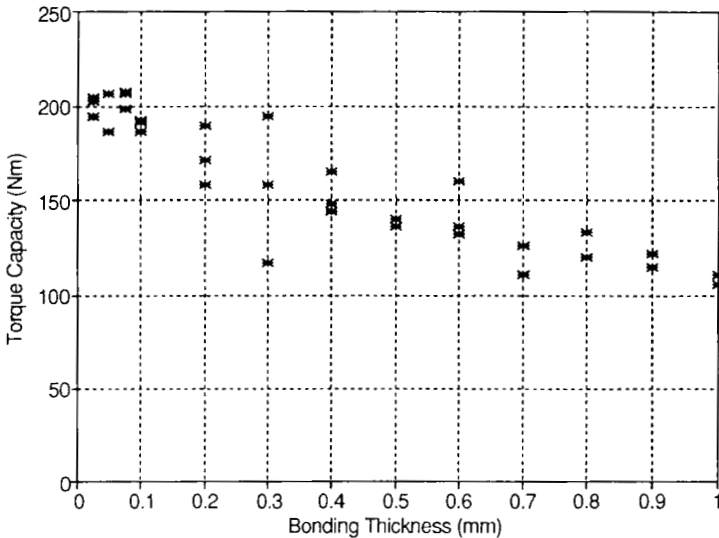


FIGURE 4 Experimentally determined static torque capacity of the adhesively bonded tubular single lap joints.

Downloaded At: 13:50 22 January 2011

Figure 4 shows the static torque capacity of the adhesively bonded tubular single lap joint with respect to the adhesive layer thickness. The static torque capacity of the joint was almost constant when the adhesive thickness was in the range of 0.02~0.1 mm.

The near-constant torque capacity when the adhesive layer thickness was less than 0.1 mm might be explained by the fully plastic deformation of the adhesive layer without interfacial debonding between the adhesive and the adherends until one of the adhesive ends reached the failure strain.

As the adhesive thickness increased further, the torque capacity of the joint decreased rapidly, which was contrary to the calculated results.^{2,5} The decrease of the torque capacity beyond 0.1 mm of adhesive thickness might be explained by the interfacial debonding between the adhesive and the adherends before the adhesive reached the failure strain, because the residual thermal stresses due to fabrication increase as the adhesive thickness increases.

STRESS ANALYSIS BY FINITE ELEMENT METHOD

In order to predict the torque capacity of the adhesively bonded joint, both the residual thermal stresses due to fabrication and the mechanical stresses due to torque must be calculated, because it was assumed that the joint had different failure modes according to the residual thermal stresses. If the adhesive and adherend materials have linear stiffnesses, the residual thermal stresses are decoupled from the mechanical stresses under torque because of the axisymmetric structure of the adhesively bonded tubular joint. Therefore, the residual thermal stresses due to fabrication and the mechanical stresses were calculated separately by a finite element method as follows:

(A) Analysis of Residual Thermal Stresses due to Fabrication

If the difference between the cure and test temperatures is ΔT , the constitutive equation for the residual thermal stress due to fabrication is expressed by the following equation:

$$\{\sigma^t\} = [C] (\{\epsilon^t\} - \{\alpha\}\Delta T) \quad (1)$$

where,

$\{\sigma^t\}$ = residual thermal stress due to fabrication

$[C]$ = elastic moduli matrix

$\{\epsilon^t\}$ = residual thermal strain due to fabrication

$\{\alpha\}$ = thermal expansion coefficient tensor

In analyzing the residual thermal stresses in the adhesive joint, a finite element method with linear stiffness properties was used, because the magnitudes of the residual thermal stresses due to fabrication must be less than the yield stress of the adhesive if the adhesive joint was properly manufactured.

The Garlerkin formulation of Equation (1) is as follows:¹⁴

$$\int [B]^T [C] [B] d\Omega \cdot \{u^t\} = \int [B]^T ([C] \{\alpha\} \Delta T) d\Omega \tag{2}$$

where,

$\{u^t\}$ = thermal displacement vector

$[B]$ = transform matrix from displacement vector to strain vector

Ω = volume element

In calculating the residual thermal stresses due to fabrication using Equation (2), an 8-node axisymmetric isoparametric element was used. Figure 5 shows the finite element mesh for the residual thermal stress. From the finite element analysis, σ_r^t , σ_θ^t , σ_z^t , and τ_{rz}^t were obtained and these were used to determine the failure mode of the adhesive. Figure 6 shows the residual thermal stresses calculated by the finite element method.

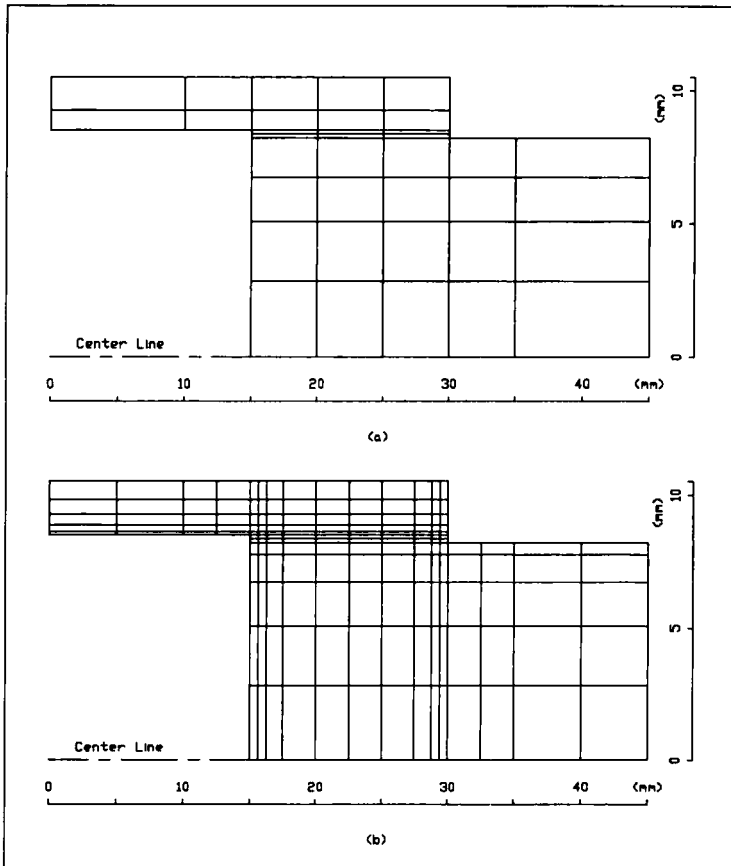


FIGURE 5 Finite element mesh for stress analysis. (a) Case of analysis of residual thermal stress due to fabrication; (b) Case of analysis of mechanical stress under torsion.

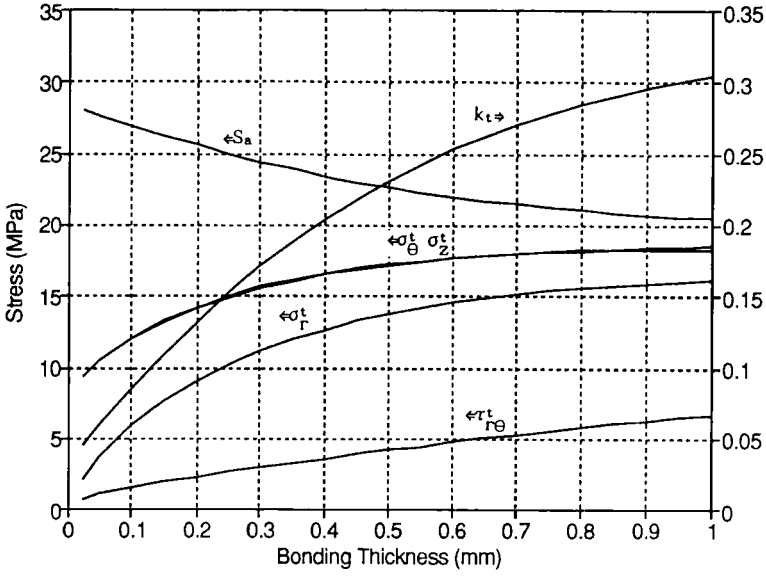


FIGURE 6 Calculated values of residual thermal stresses due to fabrication (σ_r^t , σ_θ^t , σ_z^t , and $\tau_{r\theta}^t$), reduced shear strength S_a , and nondimensionalized stress deviation factor k_t w.r.t. the adhesive thickness.

(B) Axisymmetric Mechanical Stress Analysis Under Torsion

The differential equation for the stress analysis of the axisymmetric structure under torsion can be expressed by the following equation:¹³

$$\frac{\partial}{\partial r} \left(\frac{1}{G_{\theta z}} r^3 \frac{\partial \phi}{\partial r} \right) + \frac{\partial}{\partial z} \left(\frac{1}{G_{r\theta}} r^3 \frac{\partial \phi}{\partial z} \right) = 0 \quad (3)$$

where, $G_{r\theta}$ and $G_{\theta z}$ are shear moduli for the $r-\theta$ and $\theta-z$ directions, respectively. If we define ψ to be the twisting angle, $\frac{v}{r}$, Equation (3) becomes the following:

$$\frac{\partial}{\partial r} \left(G_{r\theta} r^3 \frac{\partial \psi}{\partial r} \right) + \frac{\partial}{\partial z} \left(G_{\theta z} r^3 \frac{\partial \psi}{\partial z} \right) = 0 \quad (4)$$

$G_{r\theta}$ and $G_{\theta z}$ are expressed by the following equation:

$$G_{r\theta} = G_{\theta z} \equiv G \equiv \frac{\bar{\sigma}^m}{\bar{\epsilon}^m} \quad (5)$$

because the adhesive and the adherends used are isotropic materials, and $\bar{\sigma}^m$ and $\bar{\epsilon}^m$ are defined by the following equations:

$$\bar{\sigma}^m \equiv \left(\tau_{r\theta}^{m^2} + \tau_{\theta z}^{m^2} \right)^{1/2} \quad (6)$$

$$\bar{\epsilon}^m \equiv \left(\gamma_{r\theta}^{m^2} + \gamma_{\theta z}^{m^2} \right)^{1/2} \quad (7)$$

The Galerkin formulation of the Equation (4) was performed for the axisymmetric stress analysis of the joint under torsion.¹⁴ The nonlinear adhesive property was

incorporated through the piecewise fifth and zeroth order polynomial functions which were fitted to the curve of Figure 1, and the 8-node isoparametric element (Figure 5) was used. From the finite element analysis, the two mechanical stress terms, $\tau_{r\theta}^m$ and $\tau_{\theta z}^m$, were obtained.

FAILURE MODEL FOR ADHESIVE

The epoxy adhesive used was rubber-toughened and had very large plastic strains, especially in the shear mode, as shown in Figure 1. It was assumed that there were two kinds of failure modes of the adhesive tubular joints under torsion: One mode was that there was good bonding between the surfaces of the adhesive and the adherends and was very stable under torsion when the residual thermal stresses due to fabrication were small compared with the bulk shear strength of the adhesive. In this case, the adhesive failure occurred after the shear strain increased far beyond the yield shear strain of the adhesive. Since the shear stress of the adhesive does not increase after yielding, the shear stress saturates from the ends of the adhesive because the ends of the adhesive have maximum strains. Therefore, in this case, it was assumed that the failure of the adhesive initiated when either end region of the adhesive reached the failure strain. If all regions of the adhesive are in the plastic range and yet the adhesive end does not reach the failure strain, the torque capacity of the adhesive joint can be calculated simply by multiplying the bulk shear strength of the adhesive, the adhesive area and the mean radius from the joint axis. If the end region of the adhesive reaches the failure strain of the adhesive and yet the inside of the adhesive does not reach the yield strength of the adhesive, the torque must be calculated by the finite element method which incorporates the nonlinear material properties of the adhesive. In short, if the adhesive thickness is small enough not to induce large residual thermal stress due to fabrication, the failure of the adhesive joint is predicted by the maximum strain criterion. Therefore, in the bulk failure mode of the adhesive, the optimum bonding length of the adhesively bonded tubular lap joint is the length in which the shear strain at the end region of the adhesive reaches the failure strain and all of the inner region of the adhesive reaches the yield stress.

In the other mode, it was assumed that the bonding strength between the adhesive and the adherend was less than the adhesive bulk shear strength due to the residual thermal stress due to fabrication and they were failed at the interface between the adhesive and the adherends.

Between these two types of the failure modes, it was assumed that a transient failure existed and was defined by the transient failure mode in this paper.

In order to predict the failure condition of the interfacial failure mode, the stress failure criterion was proposed by the following equation:

$$\left(\frac{\sigma_r^t}{S_t}\right)^2 + \left(\frac{\sigma_\theta^t}{S_t}\right)^2 + \left(\frac{\sigma_z^t}{S_t}\right)^2 + \left(\frac{\tau_{r\theta}^m}{S_s}\right)^2 + \left(\frac{\tau_{\theta z}^m}{S_s}\right)^2 + \left(\frac{\tau_{rz}^t}{S_s}\right)^2 = 1 \quad (8)$$

where,

S_t = bulk tensile strength of the adhesive

S_s = bulk shear strength of the adhesive

Here we assumed that the interfacial failure mode existed when the residual thermal stresses and the mechanical stresses under torque satisfied Equation (8). Then the torque capacity of the adhesively bonded tubular lap joint was calculated using the stresses obtained by the finite element method when the stresses of the end region of the adhesive satisfied Equation (8).

In short, the torque capacity when the adhesive failed due to bulk shear failure of the adhesive was calculated by the maximum shear strain criterion while the torque capacity when the adhesive failed by interfacial failure between the adhesive and adherends was calculated by the shear stress criterion.

However, we did not know yet when the adhesive joint might be failed by the bulk shear failure of the adhesive or the interfacial failure between the adhesive and the adherends. To predict the interfacial shear failure and the bulk shear failure, we defined the reduced shear strength S_a by the following equation:

$$S_a = S_s \left[1 - \left\{ \left(\frac{\sigma_r^t}{S_t} \right)^2 + \left(\frac{\sigma_\theta^t}{S_t} \right)^2 + \left(\frac{\sigma_z^t}{S_t} \right)^2 + \left(\frac{\tau_{rz}^t}{S_s} \right)^2 \right\} \right]^{1/2} \quad (9)$$

Here, S_a represents the reduced bulk shear strength in which the effect of the residual thermal stresses was incorporated. Figure 6 shows the reduced shear strength, S_a , with respect to the adhesive thickness in which S_a decreased as the adhesive thickness increased. Also, the nondimensionalized stress deviation factor k_t was defined by the following equation:

$$k_t = \frac{S_s - S_a}{S_s} \quad (10)$$

Here k_t represents the effect of the residual thermal stress on the adhesive failure shear strength. k_t is 0 when there is no residual thermal stress and increases as the residual thermal stress increases.

In order to predict the torque capacity of the adhesively bonded tubular lap joint, we defined the transient interpolation function, f_i , by the following equation:

$$T_R = T_B * f_i + T_I * (1 - f_i) \quad (11)$$

where,

T_B : torque capacity in the bulk shear failure mode of the adhesive

T_I : torque capacity in the interfacial failure mode between the adhesive and the adherends

In order to determine the value of k_t , static torsion test results of Figure 4 were compared with the results of the finite element analysis of Figure 7. In Figure 7, there are two curves which were calculated by the two assumptions of the bulk shear failure of the adhesive and the interfacial failure between the adhesive and the adherends. From Figure 7, we can see that the torque capacity of the adhesively bonded tubular single lap joint can be calculated by the bulk shear failure when the adhesive thickness is less than 0.1 mm and it can be calculated by the interfacial shear failure when the adhesive thickness is larger than 0.5 mm. From Figure 6, we can observe that k_t in this range of adhesive thickness was less than 0.085 and greater than 0.23. Therefore, it was assumed that the joints failed by the bulk shear mode

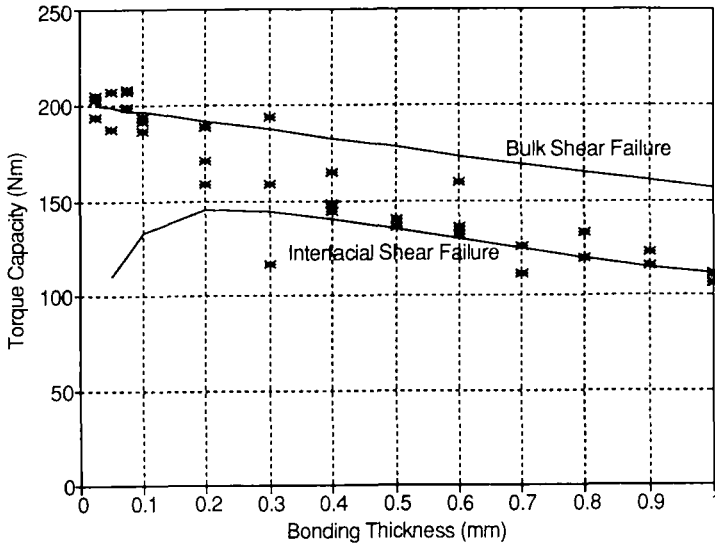


FIGURE 7 Torque capacities calculated by FEM using the bulk shear failure and interfacial shear failure of the adhesive with the experimental results of Figure 4.

when k_t was less than 0.085 and the joints failed by the interfacial shear failure mode when k_t was larger than 0.23. Between these values of k_t , it was assumed that the joints failed by the transient failure mode in which the joint failed at a stress less than the bulk shear strength but larger than the stress calculated by Equation (9).

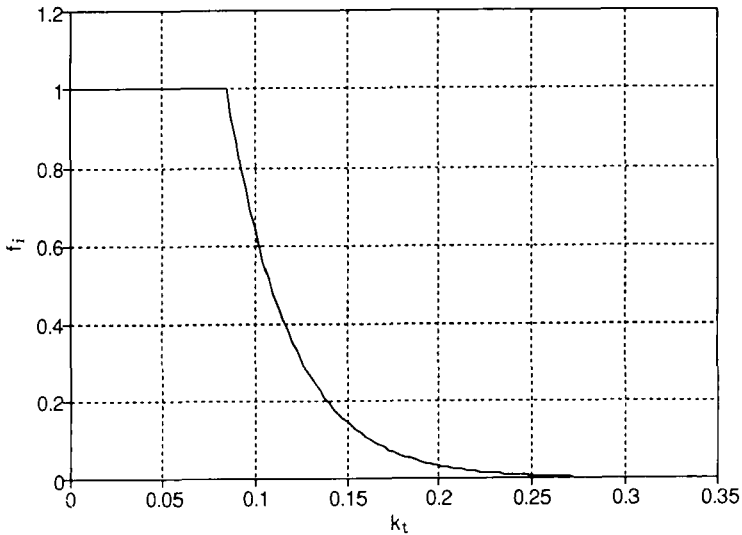


FIGURE 8 Graph of the transient interpolation function f_i versus k_t .

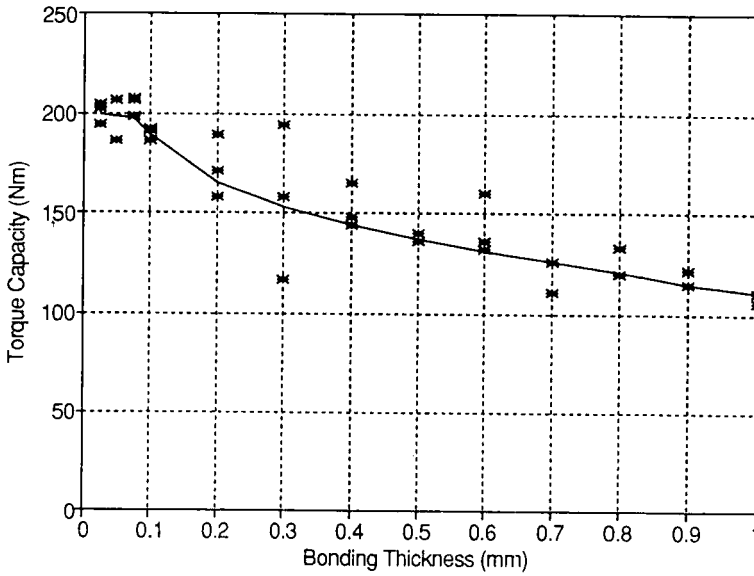


FIGURE 9 Torque capacity prediction by the transient interpolation function.

From the above results, we assumed the transient interpolation function, f_i , for the adhesively bonded tubular single lap joint with steel-steel adherends by the following equations:

$$\begin{aligned} k_t \leq 0.085 &: f_i = 1 \\ k_t > 0.085 &: f_i = e^{-29.5(k_t - 0.085)} \end{aligned} \quad (12)$$

The physical meaning of f_i is the probability of the bulk shear failure mode of the adhesive in the joint. Equation (12) includes the case where k_t is larger than 0.23 and was plotted in Figure 8.

The torque capacities calculated using Equation (11) and (12) were plotted along with the experimental results in Figure 9. We can see that the method proposed predicts well the torque capacities of the adhesively bonded tubular single lap joints.

EXTENSION TO COMPOSITE ADHERENDS

In this paper, steel adherends for the adhesive joint were experimentally tested because the control of the surface roughness was easier than for composite adherends. Since the adhesive joint is more suitable for joining composite materials to other materials, it is necessary to extend the theory to composite adherends. Using the smeared properties for the composite adherends, we can calculate the torque capacities of the joints with the composite adherends through the same procedures. However, different values of k_t and f_i will be required depending on the combinations of adherend materials. Also, an additional failure criterion to predict the

failure of the composite adherends will be required because the adhesive joint usually is designed to be statically stronger than the composite adherend.

CONCLUSIONS

The static torque capacity of adhesively bonded tubular single lap joints with steel-steel adherends was measured with respect to the adhesive thickness. It was found that the torque capacities decreased as the adhesive thickness increased, which was contrary to the results previously calculated by a closed form and a finite element method.

In order to investigate the discrepancy between the experimental torque capacity and the calculated results, a failure criterion for the adhesively bonded tubular single lap joint was proposed in which the adhesive failure mode changed from bulk shear failure, *via* transient failure, to interfacial failure between the adhesive and the adherends. To match the experimental torque capacity to the calculated torque capacity, the nonlinear shear properties of the adhesive were incorporated into the finite analysis scheme along with the proposed failure criterion.

From the experimental results and the theoretical model of the joint made with IPCO 9923 rubber-toughened epoxy, it was concluded that the adhesive joint failed in a bulk shear failure mode when the adhesive thickness was less than 0.1 mm or the nondimensionalized stress deviation factor was less than 0.085. It failed in the interfacial shear failure mode when the adhesive thickness was larger than 0.5 mm or the nondimensionalized stress deviation factor was larger than 0.23. Between these two values of adhesive thickness, it was concluded that the adhesive joint failed partly in the bulk shear failure mode and partly in the interfacial failure mode. The probability of these two failure modes in the transient failure mode was represented by the transient interpolation function.

It was proved that the proposed failure criterion for the adhesively bonded tubular single lap joints could predict well the torque capacities of the joint.

Acknowledgement

This research was financially supported by Korean Agency for Defense Development.

References

1. R. S. Alwar and Y. R. Nagaraja, "Viscoelastic Analysis of an Adhesive Tubular Joint," *J. Adhesion*, **8**, 79–92 (1976).
2. R. D. Adams and N. A. Peppiatt, "Stress Analysis of Adhesive Bonded Tubular Lap Joints," *J. Adhesion*, **9**, 1–18 (1977).
3. O. Volkersen, "Researches sur la Theorie des Assemblages Colles," *Construction Metallique*, **4**, 3–13 (1965).
4. C. T. Chon, "Analysis of Tubular Lap Joint in Torsion," *J. Composite Materials*, **16**, 268–284 (1982).
5. P. J. Hipol, "Analysis and Optimization of a Tubular Lap Joint Subjected to Torsion," *J. Composite Materials*, **18**, 298–311 (1984).
6. S. R. Graves and D. F. Adams, "Analysis of a Bonded Joint in a Composite Tube Subjected to Torsion," *J. Composite Materials*, **15**, 211–224 (1981).

7. L. J. Hart-Smith, "Further Developments in the Design and Analysis of Adhesive Bonded Structural Joints," in *Joining of Composite Materials*, **ASTM STP 749**, (1981), pp. 3–31.
8. O. T. Thomsen and A. Kildegaard, "Analysis of Adhesive Bonded Generally Orthotropic Circular Cylindrical Shells," *Developments in the Science and Technology of Composite Materials, Fourth European Conference on Composite Materials*, 723–729 (September 25–28, 1990).
9. D. G. Lee, K. S. Kim and Y. T. Lim, "An Experimental Study of Fatigue Strength for Adhesively Bonded Tubular Single Lap Joints," *J. Adhesion*, **35**, 39–53 (1991).
10. T. Smith and D. H. Kaeble, "Mechanisms of Adhesion Failure Between Polymers and Metallic Substrates: Aluminum 2024-T3 with HT 424 Adhesive," in *Treatise on Adhesion and Adhesives*, **4**, R. L. Patrick, Ed. (Marcel Dekker Inc., New York, 1981), 139–233.
11. A. J. Kinloch, *Adhesion and Adhesives* (Chapman and Hall, New York & London, 1987), 188–259.
12. F. E. Penado and K. D. Richard, "Numerical Design and Analysis," in *Adhesives and Sealants, ASTM Engineered Materials Handbook*, 477–500 (1990).
13. S. P. Timoshenko and J. N. Goodier, *Theory of Elasticity* (McGraw-Hill, New York, 1970), 341–349.
14. David S. Burnett, *Finite Element Analysis* (Addison-Wesley Publishing Company, New York, 1988), 547–684, 730–789.